HHS Public Access

Author manuscript

Macromol Biosci. Author manuscript; available in PMC 2020 June 01.

Published in final edited form as:

Macromol Biosci. 2019 June ; 19(6): e1800469. doi:10.1002/mabi.201800469.

Implantable Nanotube Sensor Platform for Rapid Analyte Detection

Eric M. Hofferber[1], **Joseph A. Stapleton**[1], **Janelle Adams**[1], **Mitchell Kuss**[2], **Dr. Bin Duan**[2], **Dr. Nicole M. Iverson**[1,*]

[1]Department of Biological Systems Engineering, University of Nebraska-Lincoln, 233 L. W. Chase Hall, Lincoln, NE 68583-0726

[2]Regenerative Medicine Program, University of Nebraska Medical Center, DRC II 6035, UNMC, Omaha, NE 68198-5965

Abstract

The use of nanoparticles within living systems is a growing field, but the long-term effects of introducing nanoparticles to a biological system are unknown. If nanoparticles remain localized after in vivo implantation unanticipated side effects due to unknown biodistribution can be avoided. Unfortunately, stabilization and retention of nanoparticles frequently alters their function. [1] In this work multiple hydrogel platforms are developed to look at long term localization of nanoparticle sensors with the goal of developing a sensor platform that will stabilize and localize the nanoparticles without altering their function. Two different hydrogel platforms are presented, one with a liquid core of sensors and another with sensors decorating the hydrogel's exterior, that are capable of localizing the nanoparticles without inhibiting their function. With the use of these new hydrogel platforms nanoparticle sensors can be easily implanted in vivo and utilized without concerns of nanoparticle impact on the animal.

Graphical Abstract

* iverson@unl.edu.

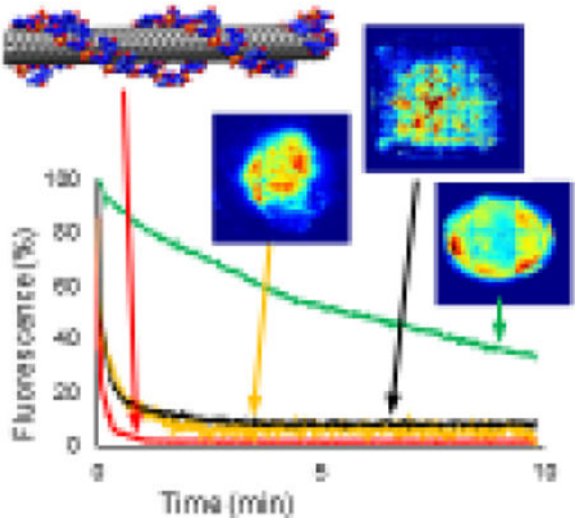

Keywords

hydrogels; biocompatibility; biomaterials; molecular recognition; nanotechnology

1. Introduction

Nanoparticles are attractive sensors for in vivo research due to their small size and large variability in sensing capabilities. Single wall carbon nanotube (SWNT) sensors are of particular interest for in vivo research due to their photostability, emission wavelength and biocompatibility.[2] SWNT have been shown to maintain their fluorescent signal over an extended period of time despite exposure to light,[3] fluoresce in the near infrared (nIR) region, where minimal light is absorbed by blood and water,[4] and be biocompatible for both in vitro and in vivo applications.[5]

Despite their many advantages, there are drawbacks in the use of SWNT in vivo. One complication for SWNT sensors is that fluorescent signals lose intensity as they travel through multiple layers of cells/tissue.[6] Another complicating factor is that due to their small size, SWNT sensors that are placed subcutaneously will diffuse away from the region of interest. The diffusion of the subcutaneous sensors occurs in a non-uniform, non-reproducible manner, making them difficult to use for long-term detection. Because of these limiting factors, the localization of SWNT sensors to a deliverable and implantable platform is required to improve long term sensing capabilities.

Hydrogels have been shown to be biocompatible, maintain stability, and allow light penetration, making them ideal candidates for a sensor delivery platform.[5c, 6–7] An alginate hydrogel was developed to localize $(AAAT)_7$ wrapped SWNT (a nitric oxide sensor) in a mouse model and was shown to be stable for 300 days following subcutaneous implantation.[5c] The encapsulation of the sensor within the hydrogel did not change the specificity of the sensor, but it did alter the rate of detection and recovery.[5c] It is hypothesized that the rate change occurred due to interactions of the SWNT's single-stranded DNA (ssDNA) wrapping

with the gel matrix. In this paper we will utilize new methods for SWNT sensor stabilization to determine which of these factors is responsible for altering sensing rates while developing a biocompatible, implantable system to localize nanoparticles without altering their intrinsic properties.

2. Experimental Section

2.1. $(AT)_{15}$ Wrapped SWNT

SWNT purchased from Sigma Aldrich ((6,5) chirality, 0.7–0.9 tube diameter, carbon <95 %, >93% carbon as SWNT) was suspended with a $d(AT)_{15}$ or a biotin-modified $d(AT)_{15}$ sequence of ssDNA (Integrated DNA Technologies) using previously developed methods.[1, 8] Briefly, SWNT and ssDNA were added in a 2:1 DNA:SWNT mass ratio to NaCl in nanopure water (0.1 M) (normal saline). The suspension was sonicated for 20 minutes with a bath sonicator (Bransonic, M2800H) followed by ultrasonication with a 3 mm probe tip sonicator (QSonica Q125 Sonicator) for 40 minutes. Suspension was centrifuged (Beckman Coulter Microfuge 16) for 180 min at 16,100 RCF and the supernatant was collected and stored at 4 C. Concentration of the SWNT-ssDNA solution was obtained via UV-Vis (Beckman Coulter, DU 730) and diluted with normal saline to obtain experimental concentrations.[8]

2.2. Fabrication of Alginate/SWNT Composite Hydrogel (AC)

SWNT sensors were encapsulated within alginate as previously described.[1, 9] Briefly, $d(AT)_{15}$–SWNT suspension (10 mg L^{-1}) was added to alginate (Nova-Matrix, PRONOVA SLM 20, 3% w/v) to form a final 2% w/v alginate solution. Alginate-SWNT suspension was crosslinked by $BaCl_2$ in nanopure water (0.1 M) ($BaCl_2$ solution) in dialysis tubes (Thermo Scientific, Slide-A-Lyzer 2000 MWCO). Hydrogels were stored in normal saline at 37 °C.

2.3. Fabrication of Alginate Liquid-Core Hydrogel (ALC)

SWNT sensor solution was encapsulated in alginate (Nova-Matrix, PRONOVA SLM 20) using three square molds (Stratasys Objet500 3D printer, material: RGD450) (see Supplemental figure 1). SWNT-ssDNA (30 mg L^{-1}) was deposited into mold 1 and frozen at −80 C. $BaCl_2$ was deposited into mold 2 and frozen at −80 °C to form two $BaCl_2$ halves. Frozen SWNT was placed between $BaCl_2$ halves and stored at −80 °C. Mold 3 was partially filled with 2% w/v alginate and SWNT-$BaCl_2$ core was placed on top of the alginate. Mold 3 was filled with 2% w/v alginate and crosslinked in a $BaCl_2$ bath. Hydrogels were either unaltered or trimmed to 8 mm x 8 mm x 8 mm. Hydrogels were stored in normal saline at 37 °C.

2.4. Fabrication of Hyaluronic Acid Liquid-Core Hydrogel (HALC)

SWNT sensor solution was encapsulated with methacrylated hyaluronic acid (HA) via extrusion printing (EnvisionTec, 3D-Bioplotter). HA and gelatin (Nova-Matrix, Pharma grade 80, Sigma-Aldrich, Gelatin from bovine skin) were dissolved separately at 5% w/v in phosphate buffered saline (PBS). Methacrylic anhydride was added to HA and gelatin solutions and allowed to react for 6 and 1 hour periods respectively. Resulting solutions were dialyzed against nanopure H_2O for 3 days and solutions were lyophilized. Hydrogel

precursor solution was prepared by dissolving methacrylated HA and methacrylated gelatin at 5% w/v in H_2O and adding a photoiniator at 0.5% w/v to induce crosslinking of polymer strands. A 1×1cm square containing a square compartment was developed with CAD (Autodesk, AutoCAD) and imported to the Bioplotter. Hyaluronic acid was loaded into the bioplotter extrusion head and the design was printed with UV crosslinking during a 30 second pausing after every second layer. After formation of the compartment, but before the top of the hydrogel was printed, a frozen SWNT solution (10 mg L^{-1}) square was deposited into the void. Solution was frozen in order to provide structural support for final two layers prior to crosslinking. After the final two layers of HA were deposited on top of the compartment, the entire hydrogel was crosslinked with UV light for 60 minutes. An identical procedure was followed for a second design consisting of a 1 cm x 1 cm square with two smaller rectangular compartments. Hydrogels were stored in normal saline at 37 °C.

2.5. Fabrication of Surface-Tethered Alginate Hydrogel (STA)

A previously published procedure by Sultzbaugh and Speaker[10] was altered to tether the SWNT sensors externally to an alginate gel. Alginate was crosslinked for 24 hours with spermine (1% w/v) in HCl solution (0.2 M) (Sigma-Aldrich) using dialysis tubes (Thermo Scientific, Slide-A-Lyzer 2000 MWCO). Hydrogels were placed in an EDC/NHSS/Avidin (Sigma-Aldrich, N-(3-Dimethylaminopropyl)-N'-ethylcarbodiimide, N-Hydroxysuccinimide, Avidin from egg white, 4 μM) bath for 16 hours at 37 °C followed by a 16 hour biotinylated SWNT-$d(AT)_{15}$ (10 mg L^{-1}) bath at 37 °C. Ratios of 1:0, 2:1, and 1:1 biotin-modified $d(AT)_{15}$ to $d(AT)_{15}$ were used for the SWNT bath. Hydrogels were stored in normal saline at 37 °C.

2.6. Hydrogel Stability

Hydrogel/sensor complexes were tested for stability by measuring size, sensor leaching, and fluorescence intensity at 990 nm. At days 0, 7, 14, 28, and 56 the normal saline bath in which the hydrogels were incubated was removed and analyzed via UV-Vis (Beckman Coulter, DU 730) to find the concentration of all SWNT, either fluorescent or non-fluorescent, in the solution.[8] An electronic caliper (Fisher Scientific, Traceable digital caliper) was used to precisely measure the dimensions of the hydrogels. Images of hydrogel platforms were captured to determine largescale physical degradation. Fluorescence intensity of the hydrogel/SWNT complex was determined using a custom-built near IR (nIR) hyperspectral microscope, similar to a previously developed system.[11] Briefly, samples were excited by a 561 nm laser, emission passed twice through a volume Bragg grating to reduce bandwidth and specify wavelength, and intensity was recorded pixel-by-pixel with an InGaAs camera (Xenics, Xeva-1.7–320 TE3).

2.7. Sensor Response to Analyte

Sensitivity and reactivity of the hydrogel sensors to an analyte was determined using the custom-built nIR microscope. NO solution was created by bubbling gas through an oxygen free, gastight flask containing normal saline and concentration was determined by electrochemical probe. Resulting NO solution was diluted to 600 μM in preparation for addition to sensing platforms. NO solution was delivered (10% v/v, final concentration of 60

μM) to each sample via gastight syringe and distance between injection and hydrogel was kept consistent. The fluorescence was continuously monitored for 10 minutes at 5 frames per second. An in-house developed program was used to analyze sample intensity over time. Sensitivity of each new hydrogel platform was compared to the previously employed AC hydrogels and free floating $(AT)_{15}$-SWNT in normal saline (FF SWNT) (10mg L^{-1}) to determine effectiveness of platform design on reactivity of sensors to the target analyte.

3. Results and Discussion

3.1. Hydrogel Sensor Development

The three new hydrogel platforms, along with the previously developed alginate composite hydrogel (AC), were fabricated and observed for changes in size and fluorescence intensity (a schematic of hydrogel fabrication is presented in Supplementary figure 2). Figure 1 (a–d) shows representative images of the four types of sensor platforms with an accompanying image showing the SWNT intensity. The SWNT fluorescence images were recorded across the nIR spectrum, but only the intensity at 990 nm, the characteristic fluorescence wavelength for 6,5 SWNT, was extracted and displayed (for full spectra see Supplementary figure 3). The 990 nm images allow conclusions about the homogeneity of SWNT distribution within each hydrogel to be drawn by highlighting major differences in fluorescence intensity, a more even color throughout the image indicates even SWNT distribution whereas appearance of dark red color indicates high aggregation of sensors compared to the hydrogel as a whole. AC (Figure 1a) and surface-tethered alginate hydrogels (STA) (Figure 1d) display 990 nm fluorescence evenly across the gel, while alginate liquid-core (ALC) (Figure 1c) and hyaluronic acid liquid-core (HALC) (Figure 1b) hydrogels show 990 nm fluorescence localized to central compartments. Emission at 990 nm indicates SWNT sensors were successfully incorporated in each hydrogel platform.

The ALC hydrogels exhibit a non-uniformity in SWNT dispersion, indicated by the dark red spot in the core, whereas the other three gels repeatedly demonstrate even SWNT fluorescence intensity throughout the region of interest. Because of the lack of uniformity and reproducibility the ALC hydrogels are not ideal for future in vivo use.

3.2. Hydrogel Sensor Stability

The AC hydrogel has previously been shown to maintain its stability when implanted subcutaneously in a mouse model for 300 days.[1] In an attempt to avoid 300 day in vivo studies for all of the new hydrogel platforms, the new complexes were compared to the AC hydrogel in vitro. Hydrogels were stored in normal saline (0.1 M NaCl) at 37 C to mimic in vivo conditions throughout stability testing. Measurement of hydrogel width and thicknesses showed no significant difference between the AC gels and the other delivery platforms except for day 14 ($p<0.05$ with one-way ANOVA), for which the AC gel showed an increase in size (Figure 2a). Swelling of hydrogels following the removal of chemical cross-linking agents is a common phenomenon,[12] and is believed to be the reason for the observed increase in gel size. The STA and the liquid-core hydrogels displayed less swelling than the AC hydrogel, presumably due to the different crosslinking agent and ability of the gel to swell inwards as well as outwards with the presence or absence of a liquid core, respectively.

Despite physical stability of the hydrogel-sensor complex, the fluorescence intensity of the sensors within the hydrogels decreased over the 56 day period (Figure 2b). In an attempt to determine whether the fluorescent signal decrease was due to a loss of nanoparticles, the storage saline of the hydrogels was tested for the presence of either fluorescent or non-fluorescent SWNT using a method previously shown by Attal et al. in which the absorption of the solution at 273 nm is used to quantify total SWNT concentration.[13] The concentration of SWNT within the storage saline was non-detectable, leading to the conclusion that the observed loss of fluorescence within the hydrogel/SWNT complex was due to a loss of SWNT fluorescence, not a decrease in the number of SWNT within the hydrogel. Since SWNT do not photobleach, we propose that the decrease of SWNT fluorescence could result from SWNT interactions/binding with the hydrogel polymer or other SWNT, both of which lead to signal quenching. It is possible that the loss of SWNT fluorescence observed in these trials is specific to DNA wrapped SWNT and will not be an issue with other fluorescent nanoparticles.

All four hydrogel platforms showed similar changes in SWNT fluorescence over time, leading to the hypothesis that the three new SWNT delivery platforms will show similar in vivo longevity as the previously tested AC platform.

3.3. Analyte Reaction Rate

Free-floating SWNT sensors (FF SWNT) in saline and all hydrogel sensor platforms were exposed to the target analyte and the fluorescence at 990 nm was recorded for a 10 minute period (Figure 3a). The SWNT sensors in this study are turnoff sensors, the fluorescence is expected to decrease in response to the addition of a target analyte. Percent fluorescence is utilized to compare the fluorescence intensity of the gels since incorporation of the SWNT with the different gels leads to different levels of signal attenuation, specifically the internal vs external SWNT will receive different levels of excitation and have different lengths of wavelength paths for emission signal detection. As previously shown, the FF SWNT fluorescence was quenched rapidly in the presence of the target analyte, quenching 99.9% of the initial fluorescence intensity.[8, 14] The fluorescence of the HALC and STA hydrogels reacted similarly to the target analyte, quenching 99.9% and 97.3% respectively. AC and ALC hydrogels fluorescence quenched to a lesser extent, only quenching 95.3% and 80.2% within the 10 minute time period ($p<0.05$). The time to reach steady state for the SWNT in solution, HALC, and STA hydrogels were comparable, reaching steady state within 30 seconds of analyte exposure ($p>0.05$). The AC and ALC hydrogels had a significantly slower reaction rate, reaching steady state around 10 minutes and 8 minutes respectively ($p<0.05$). The maximum quenching value, time to ready steady state, and effective quenching rate of the platforms are compared in Table 1. As previously shown, the AC hydrogels decrease sensitivity of the SWNT to the target analyte and for both the AC and ALC hydrogels the maximum quenching value, time to reach steady state, and effective quenching rate are all significantly different ($p<0.05$) from the desired response of FF SWNT. HALC gels were not significantly different ($p>0.05$) from FF SWNT in any category, displaying a similar rapid response to the addition of the target analyte. STA gels did have a significantly different quenching rate from the FF SWNT ($p<0.05$), but the

maximum quenching value and time to steady state were not significantly different from FF SWNT ($p>0.05$).

HALC hydrogels display similar quenching rates to the desired response of FF SWNT to addition of the target analyte. STA hydrogels show similar quenching values and time to steady state when compared to FF SWNT, but do not show a similar quenching rate to addition of the target analyte. The slower quenching rate of the STA gels could be do to incorporation of non-tethered SWNT sensors to the gel matrix.

We propose that the sensor quenching rate, and therefore maximum quench value within the 10 minute test period, is dependent on the SWNT's interaction with the hydrogel. The SWNT in the STA gels did not directly interact with the hydrogel, instead there was a linker chain that bound the SWNT wrapping to the hydrogel. Similarly, a large volume of liquid within the core of the HALC gels allowed the majority of the SWNT to avoid physically interacting with the gel. The AC gel configuration allowed direct physical contact between the hydrogel material and the sensor, changing the ability of the sensor to interact with the analyte and therefore altering the sensor quenching rate. We hypothesized that the ALC gel was interacting with the sensor in a manner similar to that observed for the AC gel because of the small volume to surface area ratio of FF SWNT contained within the liquid core.

The importance of the volume to surface area ratio was tested with HALC gels, one with a large volume to surface ratio and the other with a small ratio. The previously described HALC gel is used for the high volume to surface ratio gel and a hyaluronic acid gel with two liquid cores (2HALC) is used for the small volume to surface ratio gel. By dividing the liquid core of the HALC gel a decrease in sensor volume occurs while increasing the surface area between the sensor and the gel. Testing of the HALC and 2HALC showed that the change in volume to surface area ratio significantly changed the fluorescence quenching rate (Figure 3b), with more interaction between the sensor and hydrogel leading to a slower quenching rate after the gels' exposure to an analyte solution.

These results show the ability to tune liquid core hydrogel sensor platforms. If a project requires real time feedback on analyte detection a large volume to surface area system can be utilized, but if a decreased number of readings to provide data about a larger span of time is preferred the volume to surface area ratio can be decreased.

3.4. Time to Sensor/Analyte Interaction

Small analytes, such as NO, have very high diffusion rates.[15] With the relatively large pore size, 5 nm for alginate and 5–12 nm for hyaluronic acid,[16] of the hydrogels in comparison to NO it was hypothesized that NO would diffuse through the hydrogel quickly and the initial distance between the analyte and sensor would not be a rate determining factor in SWNT response. In order to quantify diffusion limitations for the hydrogel sensors, a second version of ALC hydrogel was made, one with a larger hydrogel wall of 4 mm (thick ALC) than its counterpart with a wall of 2 mm (previously described ALC, which will be labeled thin ALC for this set of experiments). There was a significant difference in the SWNT quenching rate for the thin and thick ALC gels as shown in Figure 4a. Extrapolation of the quenching curves predicts that the thick ALC gel will take 66.3 minutes to reach steady

state, whereas the thin ALC gel only took 7.5 minutes to reach steady state (Figure 4b) ($p<0.05$). The trend of gel thickness correlating to the time to reach steady state continues to hold true for the HALC gels, which similarly showed that a thicker hydrogel shell (2 mm, labeled thick HALC) took longer to quench than its thinner counterpart (previously described HALC gel which has a shell of 0.4 mm thickness, labeled thin HALC gel for this experiment) ($p<0.05$).

The comparison of the thick and thin hydrogels proves that sensors encapsulated within a hydrogel can have altered quenching rate due to the hydrogel alone, independent of the activity of the sensors. The change in time to reach steady state caused by hydrogel shell thickness provides another way to optimize a sensor platform to fit experimental needs.

3.5. Range of Response

The importance of the sensor's freedom for movement and interactions was probed to see if physically constraining the SWNT changes its sensing characteristics. The STA hydrogel platform provides the opportunity to slightly alter the sensor's movement by altering the points of attachment between the sensor and the hydrogel surface. The average length of the SWNT sensors post sonication is ~150 nm,[4, 17] with an average of 10 $(AT)_{15}$ strands wrapped around each nanotube.[8, 17b, 18] By altering the $(AT)_{15}$ wrappings so that only a portion of the wrappings attach to the hydrogel surface a change in the sensor's freedom of movement can be achieved.

It was determined that altering the number of points of attachment between the sensor and hydrogel did not change the time to steady state, but it did alter the maximum quenching value. Three different compositions of STA gels were tested, one with all $(AT)_{15}$ wrappings attaching to the hydrogel (1:0 ratio of attached to non-attached), one with two thirds of the $(AT)_{15}$ wrappings attached to the hydrogel (2:1 ratio of attached to non-attached), and one with half of the $(AT)_{15}$ wrappings attached to the hydrogel (1:1 ratio of attached to non-attached, the previously discussed STA gels). The data shows that increasing the points of interaction between the sensor and the hydrogel surface decreases SWNT quenching (Figure 5a). It is hypothesized that constraining the sensor by having more points of attachment to the nanotube leads to the smaller quenching value. Decreasing the quenching value without increasing the microscope sensitivity results in a decrease in the sensitivity to changes in analyte concentration (Figure 5b). Therefore, increasing a sensor's range of movement leads to a more sensitive system. The quenching curve for the 2:1 STA hydrogel has more noise when compared to the other quenching curves. The three trials used to find the 2:1 STA average had more deviation and also did not provide as strong of a signal as the other STA hydrogels. When converting signal from a.u. to percentage the noise is amplified. The lower signal is due to a lower homogeneity in ssDNA wrapping distribution when compared to the 1:0 and 1:1 hydrogels.

4. Conclusions

Three novel hydrogel systems have been fabricated and characterized to improve sensitivity and reactivity of $(AT)_{15}$ wrapped SWNT sensors that are localized with an implantable platform. Utilizing the unique characteristics of the gels allowed for the determination of

multiple ways to alter and optimize sensor platforms to fit specific requirements. The quenching rate for the liquid core sensors depends on their volume to surface area ratio and the thickness of the outer hydrogel shell. The alginate based liquid core system is hindered by a lack of even sensor distribution and reproducibility, but a large number of gels can be quickly produced. The hyaluronic acid based liquid core system provides reproducible gels with an even distribution of the sensor, but the production of each gel requires a bit more time than its alginate counterpart.

While the surface tethered alginate gels consistently react at a fast rate to analyte exposure the range of sensing can be altered by changing the sensor's degrees of freedom. This alginate gel allows for the production of a large number of gels in a short amount of time while maintaining a fast reaction time similar to the free floating sensors.

Between the tunability of sensor response through alteration of the hydrogel platform and the long term stability of all three of the new hydrogels described, multiple systems for in vivo sensing have been developed. The sensors used in this research react to nitric oxide, but SWNT can be used as sensors for a number of other analytes by changing its polymer wrapping.[19] It is possible to extend the use of the sensing platforms even farther by using other, non SWNT based sensors with these hydrogels.

The world of nanotechnology thrives on the development and use of small systems, but when a sensor needs to be stabilized in vivo going smaller is not always optimal. This research has shown three different sensor delivery platforms that allow nanoscale sensors to be utilized in vivo for extended periods of time without loss due to the migration of nanoscale systems.

Supplementary Material

Refer to Web version on PubMed Central for supplementary material.

Acknowledgements

We would like to thank the Nebraska Center for Integrated Biomolecular Communication (NIH National Institutes of General Medical Sciences P20-GM113126) for funding this project.

Abbreviations

SWNT	Single-walled carbon nanotube
nIR	Near infrared
ssDNA	Single-stranded DNA
NO	Nitric oxide
AC	Alginate composite
ALC	Alginate liquid-core
HALC	Hyaluronic acid liquid-core

STA	Surface-tethered alginate
FF SWNT	Free floating SWNT

References

[1]. Iverson NM, Barone PW, Shandell M, Trudel LJ, Sen S, Sen F, Ivanov V, Atolia E, Farias E, McNicholas TP, Reuel N, Parry NMA, Wogan GN and Strano MS, Nature Nanotechnology 2013, 8, 873.

[2]. a) Wray S, Cope M, Delpy DT, Wyatt JS and Reynolds EOR, Biochimica et Biophysica Acta (BBA) - Bioenergetics 1988, 933, 184–192; [PubMed: 2831976] b) Kruss S, Hilmer AJ, Zhang J, Reuel NF, Mu B. and Strano MS, Advanced Drug Delivery Reviews 2013, 65, 1933–1950; [PubMed: 23906934] c) Liu Z, Tabakman S, Welsher K. and Dai H, Nano Research 2009, 2, 85–120; [PubMed: 20174481] d) Graff RA, Swanson JP, Barone PW, Baik S, Heller DA and Strano SM, Advanced Materials 2005, 17, 980–984.

[3]. Heller DA, Baik S, Eurell TE and Strano MS, Advanced Materials 2005, 17, 2793–2799.

[4]. O'Connell MJ, Bachilo SM, Huffman CB, Moore VC, Strano MS, Haroz EH, Rialon KL, Boul PJ, Noon WH, Kittrell C, Ma J, Hauge RH, Weisman RB and Smalley RE, Science 2002, 297, 593–596. [PubMed: 12142535]

[5]. a) Wu W, Wieckowski S, Pastorin G, Benincasa M, Klumpp C, Briand JP, Gennaro R, Prato M. and Bianco A, Angew Chem Int Ed Engl 2005, 44, 6358–6362; [PubMed: 16138384] b) Kam NWS, O'Connell M, Wisdom JA and Dai H, Proceedings of the National Academy of Sciences of the United States of America 2005, 102, 11600–11605; [PubMed: 16087878] c) Iverson NM, Barone PW, Shandell M, Trudel LJ, Sen S, Sen F, Ivanov V, Atolia E, Farias E, McNicholas TP, Reuel N, Parry NMA, Wogan GN and Strano MS, Nature Nanotechnology 2013, 8, 873–880;d) Liu Z, Sun X, Nakayama-Ratchford N. and Dai H, ACS Nano 2007, 1, 50–56; [PubMed: 19203129] e) Dumortier H, Lacotte S, Pastorin G, Marega R, Wu W, Bonifazi D, Briand JP, Prato M, Muller S. and Bianco A, Nano Lett 2006, 6, 1522–1528; [PubMed: 16834443] f) Chen X, Tam UC, Czlapinski JL, Lee GS, Rabuka D, Zettl A. and Bertozzi CR, Journal of the American Chemical Society 2006, 128, 6292–6293; [PubMed: 16683774] g) Chin SF, Baughman RH, Dalton AB, Dieckmann GR, Draper RK, Mikoryak C, Musselman IH, Poenitzsch VZ, Xie H. and Pantano P, Exper. Biol. Med. 2007, 232, 1236–1244;h) Yehia HN, Draper RK, Mikoryak C, Walker EK, Bajaj P, Musselman IH, Daigrepont MC, Dieckmann GR and Pantano P, J Nanobiotechnology 2007, 5, 8; [PubMed: 17956629] i) Schipper ML, Nakayama-Ratchford N, Davis CR, Kam NWS, Chu P, Liu Z, Sun X, Dai H. and Gambhir SS, Nature nanotechnology 2008, 3, 216–221;j) Liu Z, Davis C, Cai W, He L, Chen X. and Dai H, Proceedings of the National Academy of Sciences 2008, 105, 1410;k) Cherukuri P, Bachilo SM, Litovsky SH and Weisman RB, Journal of the American Chemical Society 2004, 126, 15638–15639. [PubMed: 15571374]

[6]. Iverson N, Bisker G, Farias E, Ivanov V, Ahn J, Wogan GN and Strano MS, Journal of Biomedical Nanotechnology 2016, 12, 1035–1047. [PubMed: 27305824]

[7]. a) Cho WJ, Oh SH and Lee JH, Journal of Biomaterials Science, Polymer Edition 2010, 21, 701–713; [PubMed: 20482979] b) Lee KY and Mooney DJ, Progress in polymer science 2012, 37, 106–126; [PubMed: 22125349] c) Ulery BD, Nair LS and Laurencin CT, Journal of polymer science. Part B, Polymer physics 2011, 49, 832–864.

[8]. Zhang J, Boghossian AA, Barone PW, Rwei A, Kim J-H, Lin D, Heller DA, Hilmer AJ, Nair N, Reuel NF and Strano MS, Journal of the American Chemical Society 2011, 133, 567–581. [PubMed: 21142158]

[9]. Iverson NM, Bisker G, Farias E, Ivanov V, Ahn J, Wogan GN and Strano MS, Journal of Biomedical Nanotechnology 2016, 12, 1035–1047. [PubMed: 27305824]

[10]. Sultzbaugh KJ and Speaker TJ, J Microencapsul 1996, 13, 363–376. [PubMed: 8808774]

[11]. Roxbury D, Jena PV, Williams RM, Enyedi B, Niethammer P, Marcet S, Verhaegen M, Blais-Ouellette S. and Heller DA, Scientific Reports 2015, 5, 14167. [PubMed: 26387482]

[12]. a) Tam SK, Dusseault J, Bilodeau S, Langlois G, Hallé J-P and Yahia LH, Journal of Biomedical Materials Research Part A 2011, 98A, 40–52;b) Lee KY, Rowley JA, Eiselt P, Moy EM, Bouhadir

KH and Mooney DJ, Macromolecules 2000, 33, 4291–4294;c) Matyash M, Despang F, Ikonomidou C. and Gelinsky M, Tissue Engineering Part C: Methods 2013, 20, 401–411. [PubMed: 24044417]

[13]. Attal S, Thiruvengadathan R. and Regev O, Analytical Chemistry 2006, 78, 8098–8104. [PubMed: 17134145]

[14]. Kim J-H, Heller DA, Jin H, Barone PW, Song C, Zhang J, Trudel LJ, Wogan GN, Tannenbaum SR and Strano MS, Nature Chemistry 2009, 1, 473.

[15]. a) Zacharia IG and Deen WM, Annals of Biomedical Engineering 2005, 33, 214–222; [PubMed: 15771275] b) Beckman JS and Koppenol WH, American Journal of Physiology-Cell Physiology 1996, 271, C1424–C1437.

[16]. a) Boontheekul T, Kong H-J and Mooney DJ, Biomaterials 2005, 26, 2455–2465; [PubMed: 15585248] b) Xu X, Jha AK, Harrington DA, Farach-Carson MC and Jia X, Soft matter 2012, 8, 3280–3294. [PubMed: 22419946]

[17]. a) Nakayama-Ratchford N, Bangsaruntip S, Sun X, Welsher K. and Dai H, Journal of the American Chemical Society 2007, 129, 2448–2449; [PubMed: 17284037] b) Zheng M, Jagota A, Strano MS, Santos AP, Barone P, Chou SG, Diner BA, Dresselhaus MS, McLean RS, Onoa GB, Samsonidze GG, Semke ED, Usrey M. and Walls DJ, Science 2003, 302, 1545. [PubMed: 14645843]

[18]. a) Jin H, Jeng ES, Heller DA, Jena PV, Kirmse R, Langowski J. and Strano MS, Macromolecules 2007, 40, 6731–6739;b) Campbell JF, Tessmer I, Thorp HH and Erie DA, Journal of the American Chemical Society 2008, 130, 10648–10655; [PubMed: 18627153] c) Harvey JD, Jena PV, Baker HA, Zerze GH, Williams RM, Galassi TV, Roxbury D, Mittal J. and Heller DA, Nature biomedical engineering 2017, 1, 0041.

[19]. a) Heller DA, Jin H, Martinez BM, Patel D, Miller BM, Yeung T-K, Jena PV, Höbartner C, Ha T, Silverman SK and Strano MS, Nature Nanotechnology 2008, 4, 114;b) Barone PW, Baik S, Heller DA and Strano MS, Nature Materials 2005, 4, 86-U16;c) Landry MP, Kruss S, Nelson JT, Bisker G, Iverson NM, Reuel NF and Strano MS, Sensors 2014, 14, 16196–16211. [PubMed: 25184487]

Novel hydrogel platforms for in vivo delivery of nanoparticle sensors are developed. Two new platforms are able to maintain nanoparticle localization without altering specificity or reaction time, thus creating stable platforms for long-term in vivo studies.

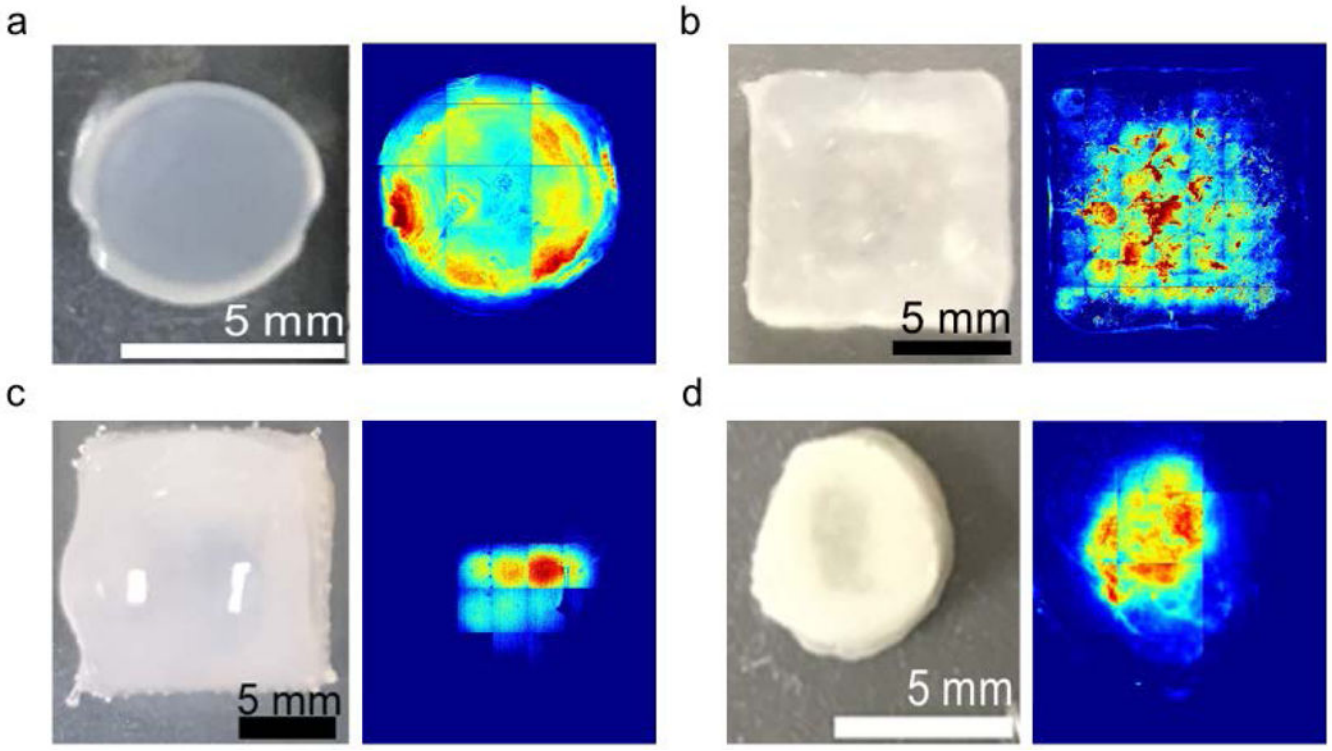

Figure 1.

Representative photographs of the four types of hydrogel-SWNT sensor platforms with accompanying fluorescence image at 990 nm. Images depicting fluorescence intensity of the SWNT sensors are shown with red representing the highest intensity and blue representing the lowest intensity normalized to each image. Fluorescence images confirm association of SWNT sensors into hydrogel platforms. a) Alginate composite: AC, hydrogels show intensity spread across the entirety of the gel; b) hyaluronic acid liquid-core: HALC hydrogels show an even distribution of intensity within the core and little to no fluorescence outside of the core (edges); c) alginate liquid-core: ALC hydrogels did show fluorescence only within the core, but fluorescence is not well distributed; and d) surface-tethered alginate: STA hydrogels show and even distribution of fluorescence across the gel.

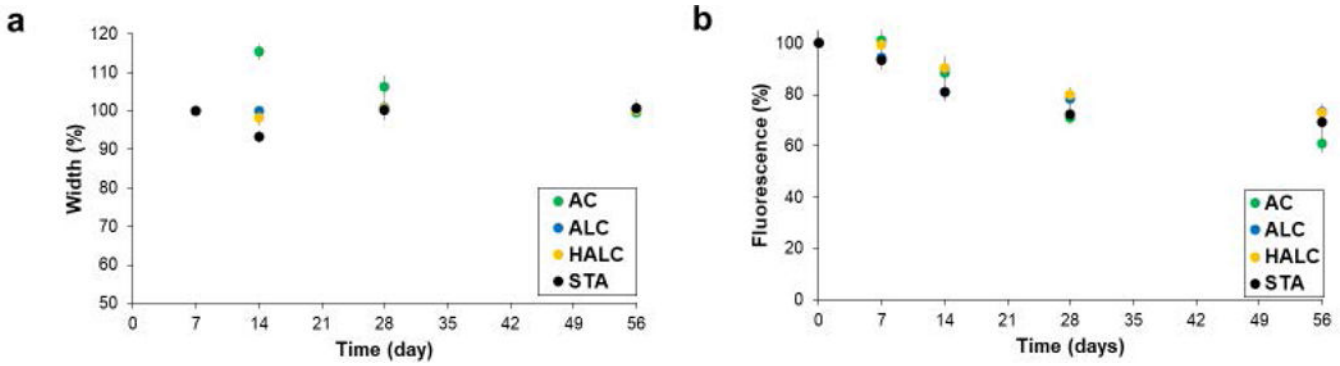

Figure 2.

Stability of the hydrogel platforms were assayed at 7, 14, 28 and 56 days post synthesis through measurement of a) hydrogel width and b) sensor fluorescence normalized to initial values. AC hydrogels show significant swelling at day 14 ($p<0.05$). All hydrogel platforms show a significant decrease in fluorescence intensity from the initial value starting at day 28 ($p<0.05$), but no platform decreased significantly more than the others ($p>0.05$). (n = 3, error bars are SEM)

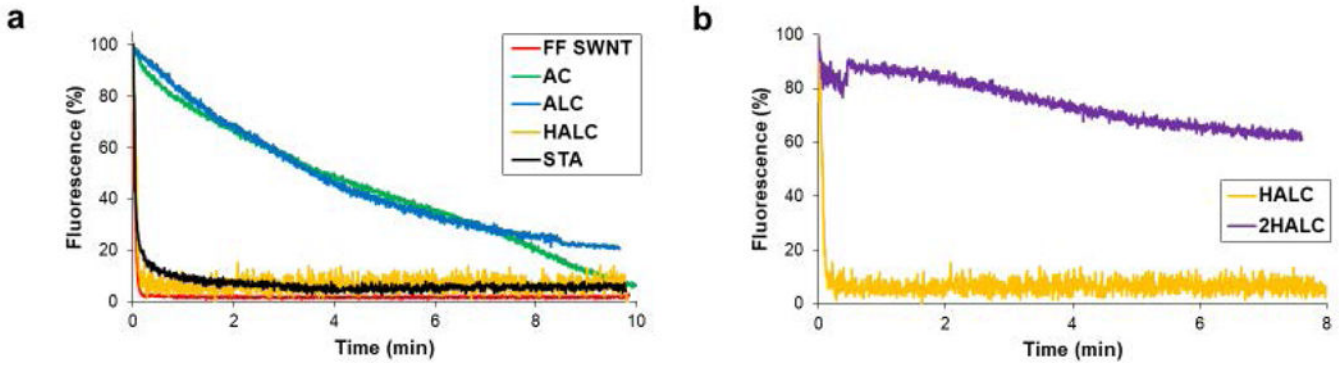

Figure 3.

SWNT sensor response to analyte exposure is dependent on the hydrogel delivery platform. Quenching curves shown are the average of three trials (n = 3). a) ALC hydrogels showed delayed sensor response similar to what is observed for the AC gel. The STA and HALC hydrogels provide a stabilization platform to localize the SWNT while allowing free sensor interaction with the analyte, leading to sensor response similar to that observed in FF SWNT. b) 2HALC hydrogels had a significantly delayed sensor response compared to HALC indicating a response rate dependence on volume to surface area ratio of liquid core hydrogels.

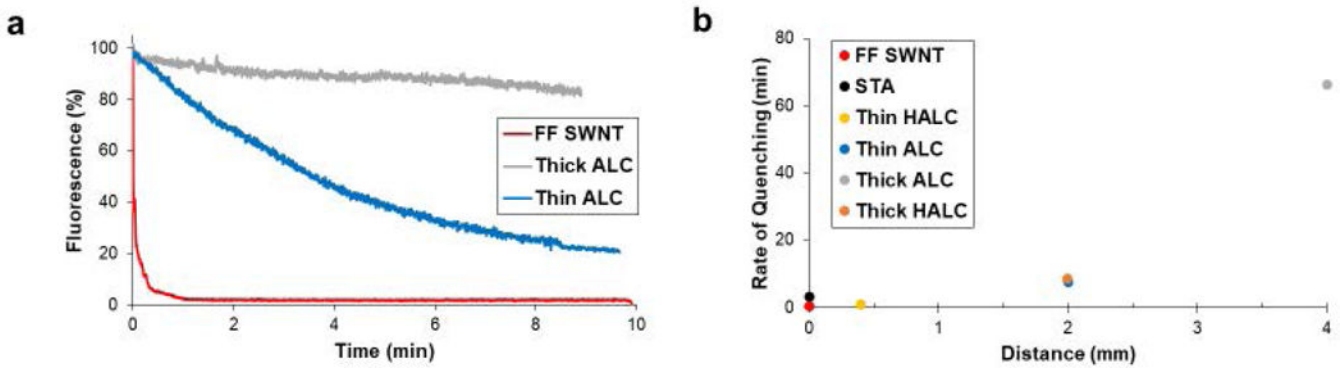

Figure 4.

a) ALC hydrogels with either a thin or thick shell were exposed to the target analyte and the fluorescence was recorded. SWNT fluorescence quenching is shown to be significantly dependent on the distance between the sensor and the analyte solution. b) Hydrogel platforms that limit the distance from sensor to analyte display faster rates of signal quenching when compared to hydrogels that have a thicker shell between SWNT sensor solution and the surface of the gel ($p<0.05$). (n = 3, error bars are SEM)

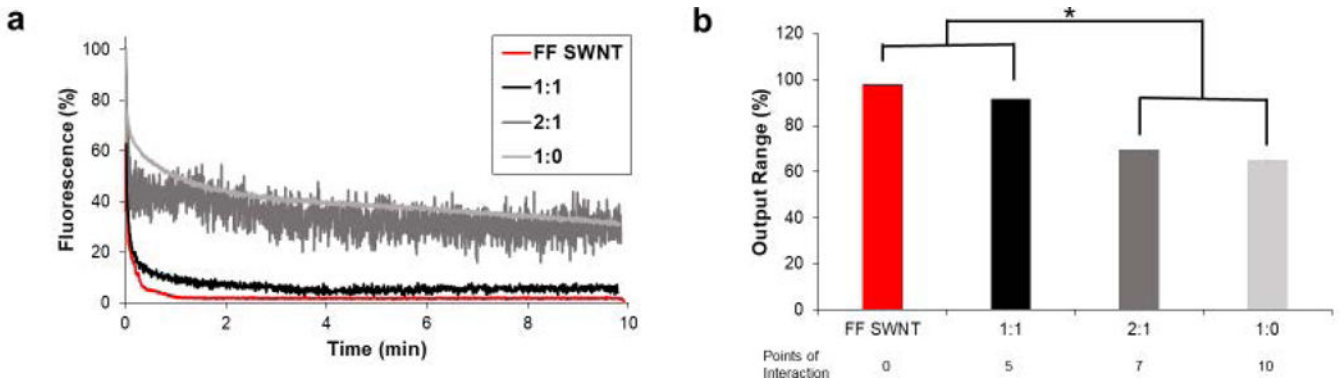

Figure 5.

Surface-tethered hydrogels were modified with varying ratios of SWNT wrapping that interacted with the hydrogel to SWNT wrapping that did not interact with the hydrogel. a) The quenching rate was similar for the different ratios of SWNT wrapping that was attached to the hydrogel, but b) the output range was significantly altered by changing the number of interaction points between the sensor and the hydrogel, with more points of contact leading to significantly smaller output ranges ($p<0.05$). The 2:1 hydrogels resulted in more noise due to a nonhomogeneous distribution of ssDNA wrappings on the nanotubes. (n = 3, error bars are SEM)

Table 1.

Fluorescence quenching is given in percentage of initial value and the time required for the fluorescence to reach a steady state value is given in seconds. The quenching rate is calculated from the quench value and the time required to reach steady state and is given in percentage quench per second. The quenching rate of the HALC platform was not significantly different from FF SWNT ($p>0.05$). The AC, ALC, and STA platforms had significantly different quenching rates from the FF SWNT ($p<0.05$), but the STA platform did not have a significantly different quench value or time to reach steady state from the FF SWNT ($p>0.05$). (n = 3)

Platform	Maximum Quenching Value [%]	Time to Steady State [s]	Quenching Rate [%/s]
FF SWNT	99.96 ± 0.04	9.87 ± 0.57	10.2 ± 0.557
AC	95.3 ± 2.66	551.2 ± 0.31	0.17 ± 0.005
ALC	80.16 ± 2.41	445.8 ± 39.97	0.18 ± 0.022
HALC	99.93 ± 0.07	10 ± 0.72	10.09 ± 0.7
STA	97.59 ± 0.17	20.53 ± 1.57	4.81 ± 0.392